Transient space-time surface waves characterization using Gabor analysis

2009 J. Phys.: Conf. Ser. 195 012009

(http://iopscience.iop.org/1742-6596/195/1/012009)

Journal of Physics: Conference Series **195** (2009) 012009 doi:10.1088/1742-6596/195/1/012009

Transient space-time surface waves characterization using Gabor analysis

L Martinez[1], N. Wilkie-Chancellier[1,3], C. Glorieux[2], B. Sarens[2] and E. Caplain[1]

[1] Université de Cergy Pontoise, ENS Cachan, UMR CNRS 8029, Laboratoire Systèmes et Applications des Techniques de l'Information et de l'Energie (SATIE), 5 mail Gay-Lussac, F 9500 Cergy-Pontoise, France
[2] Katholieke Universiteit Leuven, Laboratorium voor Akoestiek en Thermische Fysica (LATF), Celestijnenlaan 200D, B-3001 Leuven, Belgium

E-mail: nicolas.wilkie-chancellier@u-cergy.fr

Abstract. Laser ultrasonics allow the observation of transient surface waves along their propagation media and their interaction with encountered objects like cracks, holes, borders. In order to characterize and localize these transient aspects in the Space-Time-Wave number-Frequency domains, the 1D, 2D and 3D Gabor transforms are presented. The Gabor transform enables the identification of several properties of the local wavefronts such as their shape, wavelength, frequency, attenuation, group velocity and the full conversion sequence along propagation. The ability of local properties identification by Gabor transform is illustrated by two experimental studies: Lamb waves generated by an annular source on a circular quartz and Lamb wave interaction with a fluid droplet. In both cases, results obtained with Gabor transform enable ones to identify the observed local waves.

1. Introduction

Laser detection methods allow the investigation of ultrasonic transient phenomena in both space and time dimensions. Used along a two dimensional surface, laser ultrasonic leads to three dimensional (3D) space–time signal collections. Straight 3D Fourier analysis or classical high resolution signal processing methods can be used to identify the wave propagation information, however these methods are not adapted for identifying where and when the waves are generated. The 3D Gabor transform is presented in the view to quantify these transient aspects in the space–time–wave numbers–frequency domains. Two experimental studies illustrate the ability of local properties identification by Gabor transform, the first one in the case of Lamb waves generated by an annular source on a circular quartz sensor and the second one for Lamb wave interaction with a fluid droplet.

[3] To whom any correspondence should be addressed.

2. 3D Gabor transform

The Gabor transform was introduced in 1947 [1] in order to achieve a signal analysis closer to human perception of sound such as time localization of frequency components. It gave the principle of the time–frequency analysis by short-time Fourier transform (STFT), with the help of a sliding gaussian window [2-4].
The early applications dealt with audio signals and some efficient compression methods rose from the comprehension of their frequencies components time shape. The 2D Gabor transform were introduced in acoustics [5] in order to localize ultrasonic phonons in space–time domains and their conversions on a cylindrical shell. The 3D Gabor analysis presented here is both an extension to three dimensions and an improvement of the early 2D version cited above [6].

2.1. Localisation of phonons by 3D Gabor transform

The goal is to estimate the local space and time periods from propapagating waves signals and to map their amplitudes through the space–time domain. The fundamental hypothesis is that the propagating waves can be observed along a 2D surface on points referenced by their coordinates (x,y) at time t. This leads to the 3D space–time collection of the observed waves s(x, y, t). Along an infinite space and time field of view (FOW), by following the Fourier diamond [7-13], three other spaces can be deduced from the original signals s(x,y, t) (Figure 1 left) by Fourier transforming s(x,y,t):

- S(x,y,ω) is the time Fourier transform of s(x,y, t),
- N(kx,ky,t) is the space 2D Fourier transform of s(x,y,t) and
- Ksi(kx,ky,ω) is the 3D Fourier transform of s(x,y,t) along the space and time dimensions.

The 3D Gabor transform uses a small space and time cube sliding FOW prior Fourier transforming (Figure 1 right). The dimensions of these cubes will be chosen small enough in order to not overlap two successive wave packets (i.e. keep space-time resolution) and wide enough to keep enough resolution in the frequencies domains. A compromise must be reached but the sliding cube has to cover at least one wavelength in the spatial dimensions and at least one period in the temporal dimension.

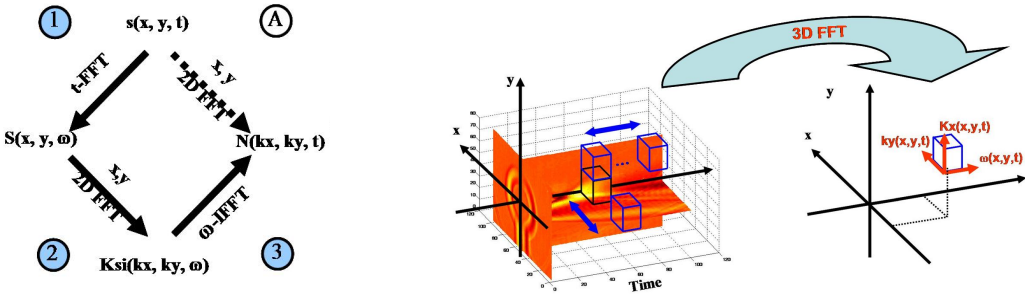

Figure 1. Fourier diamond (left) and 3D Gabor transform principle (right).

For 2D signals s(x,t), these 3 spaces have interesting properties for the modal analysis of the observed waves. The 2D Fourier transform of s(x,t) can be used to quantify, a posteriori, the wave properties, like their attenuation and phase velocities [6–13]. With the help of Prony identification, the mixed representations S(x,ω) and N(kx,t) can be also used successfully [14-15]. However when the signal s(x,t) is a sum of identical wide band wave packets delayed in time and in space, identification based on S(x,ω) allows ones to precise where the waves are packets, not when, whether N(kx,t) allows the time localization, not the space one, and Ksi(kx,ky,ω) none of both as everything is accumulated.
For 3D data signals s(x,y,t), some of the 2D tools are still usable: S(x,y,ω) is useful for identifying the wave modes. However, the problem of wide band wave localization in both time and space encountered for the 2D case remains in the 3D case, and a second difficulty appears: identification by Prony like methods is not possible without a deeper prior knowledge of the experimental signal composition [14-15].

2.2. 3D Gabor scheme

The 3D Gabor transform Z(x,y,t,kx,ky,ω) can be obtained through several equivalent paths. The first possible method is the straightforward extension of the time frequency methods STFT to three dimensional signals: a small 3D cube slides along the time and space dimensions, and the corresponding 3D spectrums Ksi(kx,ky,ω) are stacked, leading to the Z(x,y,t,kx,ky,ω) representation. However, as Z is a 6D space of complex numbers, this method needs a huge amount of computer resources to be computed and stored. Moreover the resulting Z(x,y,t,kx,ky,ω) representation is not easily readable from a physical point of view.

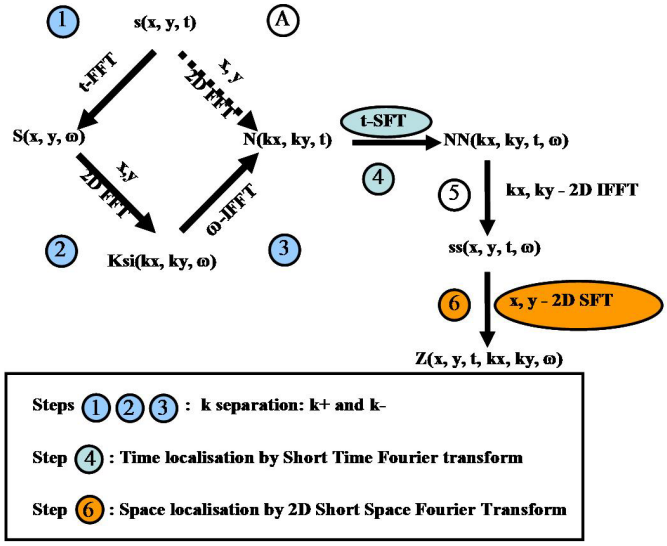

Figure 2. 3D Gabor analysis scheme and connections with the Fourier diamond spaces.

In order to reduce the computer resources needed to reach the 6D Z and to give Z a physical meaning the x, y, t localisation is done in successive steps instead of a huge one (Figure 2). The proposed scheme presented here uses the physical fact that energy flows, through the time dimension, from past to future, whereas, through the space dimensions, both directions are used. As the s(x,y,t) collection is real valued, loosing the negative frequencies that correspond to propagation towards negative time, one can orient the space propagation and separate positive wave numbers from negative ones. This is the goal of following the path (1)–(3), instead of the path (A) in Figure 3. The obtained wave number–time representation N(kx,ky,t) is then wave number oriented and the waves propagating along increasing x or y directions are separated from the one propagating in the opposite directions. The short time sliding Fourier transform (t-SFT) is then applied to N(kx,ky, t) along the time dimension (Step 4). The resulting 4D NN(kx,ky,t,ω) representation allows the localization of the wave number–frequency (kx,ky,ω) aspect through time, but still not through space. The energy localisation through space is then done by following the next two steps:

(5) NN(kx,ky,t,ω) is sent back to the space dimension by inverse space Fourier transform, leading to an intermediate space–time–frequency representation ss(x,y,t,ω),

(6) the Z(x,y,t,kx,ky,ω) representation is the short space sliding Fourier transform (x,y-2D SFT) of the ss(x,y,t,ω) representation. Instead of storing the complex values Z(x,y,t,kx,ky,ω), the wave numbers kx and ky are estimated from an identification among Z, by identifying each modulus maxima. Complex wave numbers can be extrated from the complex representation Z : the kx and ky real parts locate the peaks in Z, whereas their imaginary parts shape the peaks height and width. The real part of the wave numbers corresponds to the propagation, whereas their imaginary part represent

the attenuation coming from both the propagation and the geometry of the observed wave source (such as plane, circular). In this paper, we chose to only scan the propagation given by the real part of wave numbers. Choosing a frequency of interest x enables us to image the space–time evolution by superimposing the real part of identified wave numbers on video sequences of ss(x,y,t,ω).

3. Quartz sensor disk transients

The first application of the 3D Gabor analysis is the identification of the waves generated by an electrical pulse on a quartz sensor surface.

3.1. Quartz sensor and experimental set-up

The quartz used is a standard AT cut disk (thickness 0.3 mm, diameter 15 mm) designed to have a 6 MHz fundamental frequency (figure 3 left). The deposited gold electrodes are 5 mm in diameter. The quartz is maintained only by the electrodes and a thin chromium layer is deposited in order to impose the detection of vibration along the upper face of the quartz, with the same sensitivity, whether the laser beam is on or outside the upper gold electrode.

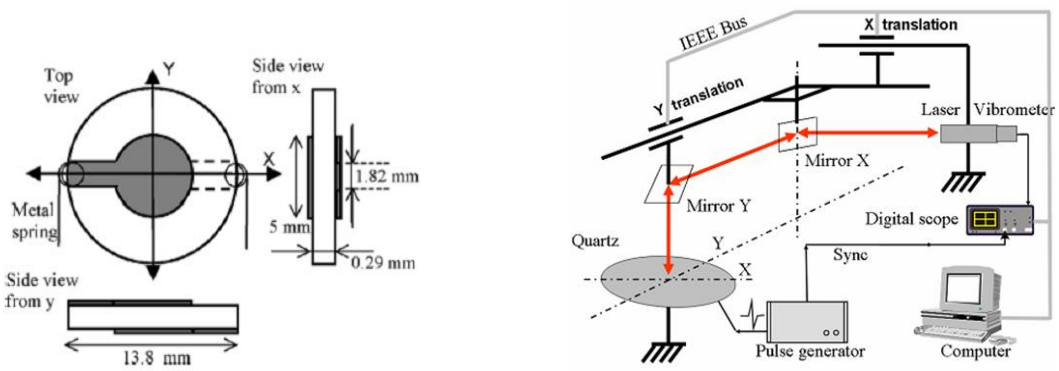

Figure 3. Quartz sensor (left) and the experimental set-up used (right)

The quartz is excited by a voltage pulse (amplitude 200 V, bandwidth 100 MHz) in order to generate waves in a wide frequency range (figure 3 right). A Polytec laser vibrometer is used for the optical detection of the acoustic waves propagating along the quartz surface. Due to the single head used, only mainly normal vibrations are measured on the quartz surface. A computer is used for both the time signal acquisition through a Lecroy digital scope and for the positioning of the laser beam through automated micro-translations.

The space acquisition is performed over rectangular area that nearly included the whole area of the quartz (80 by 110 positions, with 125 µm steps). The frequency bandwidth used is 50 MHz.

3.2. Signals and 3D Gabor analysis

Figure 4 (left) presents the space-time signals obtained by the optical detection on the upper surface of the quartz.

The snapshots in Figure 4 (right) present slices of the space-time-frequency representation ss(x,y,t,ω) for a selected frequency F = 885 kHz. The arrows lengths patched on the images are proportional to the real part, i.e. the propagating part, of the local wave numbers estimated from the 3D Gabor transform. The arrows point out the corresponding local direction of propagation.

The equivalent sliding cube used is 16x16 points along the space dimensions and 64 points along the time dimension. These values have been selected small enough in order to not overlap two successive wave packets and wide enough to keep enough resolution in the frequencies domains. In this case, the sliding cube covers one wavelength in the spatial dimensions and one period in the temporal one.

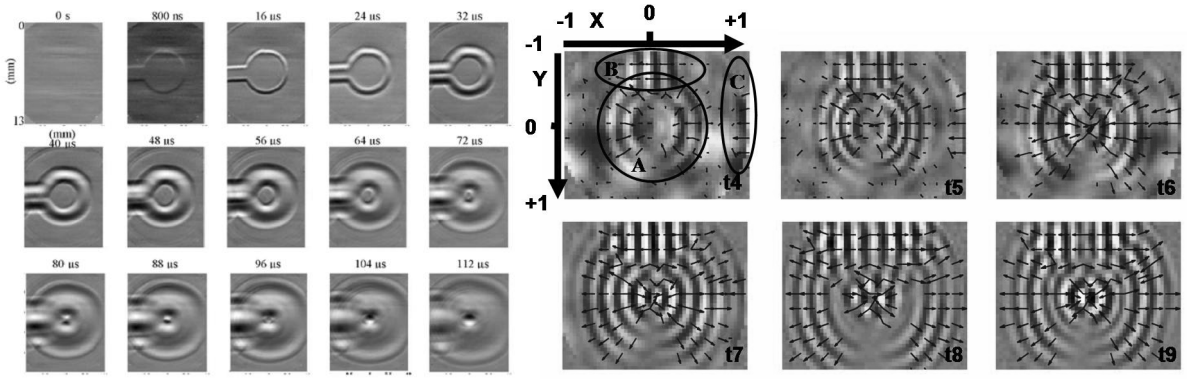

Figure 4. Space-time signals (left) and Gabor analysis at F = 885 kHz (right).

The estimated wave numbers directions confirm raw observations made from the dataset.
In zone A and B (figure 4 right), the opposite wave numbers are clearly identified for the waves generated by the electrode border. In zone A (respectively B), the circular (respectively linear) shape of the wave front is clearly shown with the radial wave numbers. For both zones, the corresponding phase velocity is close to 1770 m/s, in good agreement with experimental results presented in [16], and obtained by modal analysis. This corresponds to the A_0 Lamb mode, dispersive in this frequency domain. There is also a good agreement with the recent theoretical results presented in [17] for the flexural mode F, dispersive in this frequency domain.
In zone C, one can notice that waves are generated by the border of the quartz.
For other frequencies, A_1, S_1 and S_2 waves are identified, as their space and time generation points (Figure 5).

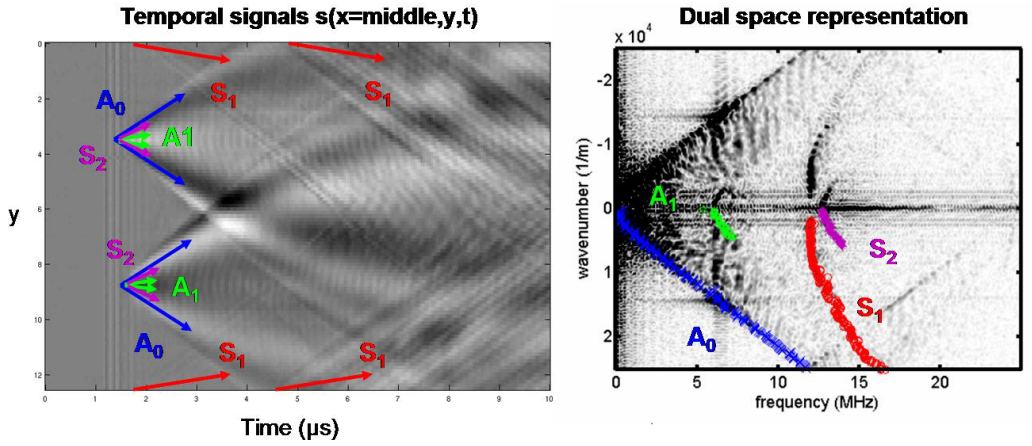

Figure 5. Identified waves for all frequencies in the spatio-temporal (left) and dual spaces (right).

4. Droplet interactions with Lamb modes

The second illustration of the 3D Gabor analysis is the interaction of Lamb waves with a fluid droplet.

4.1. Experimental set-up

In this case, a 20 µL glycerol droplet (diameter 6 mm) is put on the surface of an aluminium plate. The generation of Lamb wave is performed in pulse mode using a 2.25 MHz transducer in contact with the edge of the plate. The laser vibrometer scans a 20x20mm area surrounding the droplet, by 0.5mm

steps. A computer is used for both the time signal acquisition through the Lecroy digital scope and for positioning the laser beam through automated micro-translations.

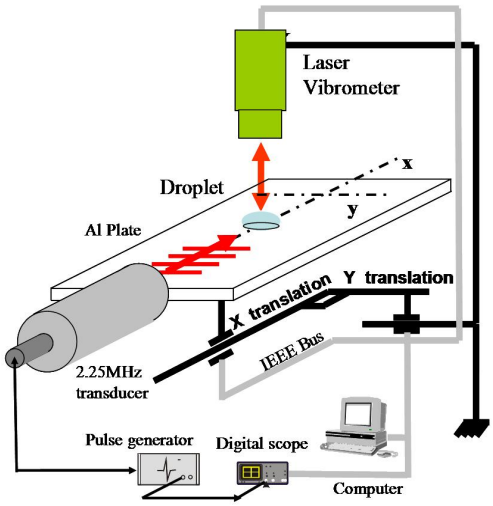

Figure 6. Experimental set-up for the study of the droplet behavior.

4.2. Signals and 3D Gabor analysis

Figure 7 (left) presents the space-time signals recorded by the optical detection on the upper surface of the aluminium plate, along the area surrounding the droplet. The interaction of the surface waves with the fluid droplet can be clearly observed.

From 3D Gabor analysis and for a selected frequency (F=1MHz), the spatio-temporal evolution of the displacements can be represented at y=0 (Figure 7 right), i.e. a cut of the previous representation. Several observations can be done. In a first hand, two different incident Lamb waves are visualized. The first generated mode is the S_0 Lamb mode and the other one is the A_0 Lamb mode. On the other hand, the interactions of the S_0 and the A_0 Lamb modes with the droplet are also observed successively.

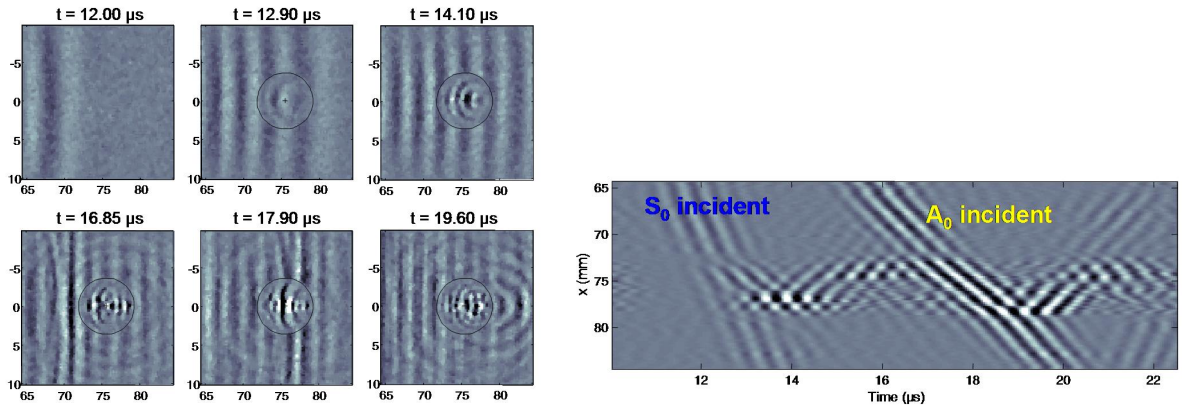

Figure 7. Space-time signals (left) and representation at y=0 (right) for F=1MHz.

The snapshots in Figure 8 are space-time-frequency representation Z(x,y,t,kx,ky,ω) for a selected frequency F = 1MHz and at several times. So, for each picture, the (kx,ky) informations are superimposed on the 2D spatial evolution s(x,y). Using this point of view, the local wavenumbers are identified [18].

On the three first snapshots, the interaction of the S_0 Lamb mode with the gycerol droplet is observed. The incident S_0 Lamb mode (t = 12.00 µs) travels under the droplet and is converted into A_0 Lamb mode and A mode at t = 12.90 µs, along the droplet border. As the A mode is a propagating mode which is characteristic of the fluid constituting the droplet, it is trapped inside and travels back and forth. The droplet focusing effect is clearly visualized on the second snapshot.The A_0 and A converted modes are propagated starting from this focal point (t = 14.10 µs).
Using the three next snapshots, the interaction of the A_0 Lamb mode with the fluid droplet can be understood. The second incident Lamb mode (A_0) is incident and converted into A mode. A second focal point can be noted starting from which the A_0 and A modes are propagated (t = 19.60 µs).

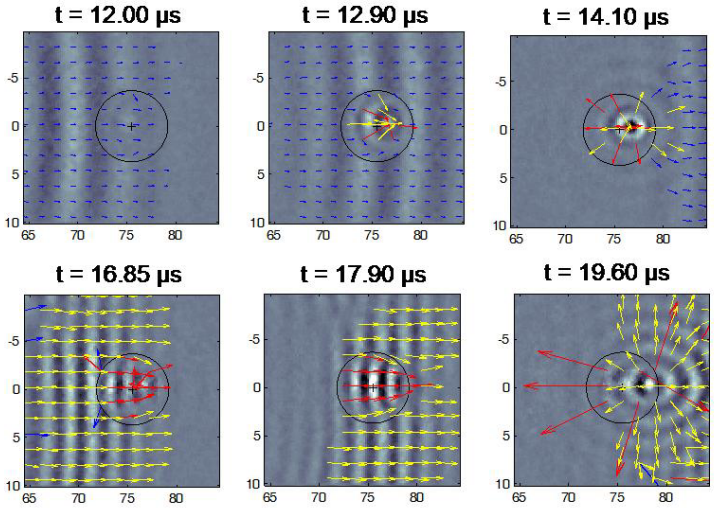

Figure 8. Space-time signals and Gabor analysis for the droplet interaction with Lamb modes at F = 1 MHz (S_0 mode in blue, A_0 mode in yellow and A mode in red)

We can note that the positions of the two focal points are not similar for t = 14.10 µs and t = 19.6 µs. This is due to the difference of velocity between the A_0 and the S_0 Lamb modes, as the refraction of the converted waves follows the Snell's law. A change of the incident wave velocity gives rise to a change of the index and then induces a change of the convergence of the converted wave along the curved droplet boundaries.
The experimental determination of the focal point position could give access to the velocity of the A mode in the droplet, and then could allow us to characterize the material constituting the droplet.

5. Conclusion

The 3D Gabor transform has been successfully employed for identifying the local wave numbers and frequencies present in transient 3D signals. The experimental results are in good agreement with theoretical modes predictions for an infinite plate.
Moreover, in the case of the quartz sensor behavior, the role played by the shape of the electrodes is clearly shown for the generation of these modes. This knowledge enables theoretical modal analysis of the real quartz sensor and to tune its electrodes shape.
In the case of the droplet study, the conversion of Lamb modes during the interaction of an incident wave with the fluid droplet allows us to monitor the droplet behavior.
Both cases pointed out that 3D Gabor transform is well adapted to the analysis of transient waves propagating with various wave fronts shapes, converting in other waves. Further investigations on non linear wave propagation cases should also give useful results.

6. References

[1] Gabor D., 1946 , Theory of communication, *Proc. Inst. Electric. Eng.*, **93 (26)** 429–457.
[2] Claasen T.A.C.M, Mecklenbraüker W.F.G, 1980, The Wigner distribution. A tool for time-frequency analysis, Part I: Continuous-time signals, *Phillips journal of research*, **35 (3)** 217-250.
[3] Claasen T.A.C.M, Mecklenbraüker W.F.G, 1980, The Wigner distribution. A tool for time-frequency analysis, Part II: Discrete-time signals, *Phillips journal of research*, **35 (3)** 276-300.
[4] Claasen T.A.C.M, Mecklenbraüker W.F.G, 1980, The Wigner distribution. A tool for time-frequency analysis, Part III: Relations with other time frequency Continuous-time signal representations, *Phillips journal of research*, **35 (6)** 373-389.
[5] Martinez L., Morvan B., Izbicki J.L., 2004, Space-time-wave number-frequency X(x,t,k,f) analysis of SAW generation on fluid filled cylindrical shells., *Ultrasonics International*, **42 (1)** 383-389.
[6] Martinez L., Goossens J., Glorieux C., Wilkie-Chancellier N., Ould Ehssein C., Serfaty S., 2006, 3D Gabor analysis of transient waves propagating along an AT cut quartz disk, *Ultrasonics International*, **43** 1173-1177.
[7] Alleyne D., Cawley P., 1991, A two-dimensional Fourier transform method for the measurement of propagating multimode signals, *J. Acoust. Soc. Am.*, **89 (3)** 1159-1168.
[8] Vollmann J., Dual J., 1997, High-resolution analysis of the complex wave spectrum in a cylindrical shell containing a viscoelastic medium. Part I. Theory and numerical results, *J. Acoust. Soc. Am.*, **102** 896-908.
[9] Vollmann J., Breu R., Dual J., 1997, High-resolution analysis of the complex wave spectrum in a cylindrical shell containing a viscoelastic medium. Part II. Experimental results versus theory, *J. Acoust. Soc. Am.*, **102** 909-920.
[10] Salisbury J.I., 1999, Wave number frequency (k-ω) analysis using wavelet transform and eigenvalue decomposition, *J. Acoust. Soc. Am*., **106 (3)** 1602–1604.
[11] Bonnet G., 1983, Au delà d'une vitesse de groupe: vitesse d'onde et vitesse de signal. Première partie: l'opérateur vitesse de groupe en l'absence d'affaiblissement, *Ann. Télécommun.*, **38 (9-10)** 1-22.
[12] Bonnet G., 1983, Au delà d'une vitesse de groupe: vitesse d'onde et vitesse de signal. Deuxième partie: déformation de l'amplitude et influence de l'affaiblissement, *Ann. Télécommun.*, **38 (11-12)**, 1-17.
[13] Martinez L., 1998, Nouvelles méthodes d'identification d'ondes de surface. Etude de l'onde A sur une cible courbe, *PhD Thesis*, Université du Havre, France.
[14] Martinez L., Duclos J., Tinel A., 1998, Aspect of cylindrical shell resonances in Fourier Diamond Spaces. Use of Surface Waves Analysis Methods (SWAM) on experimental or numerical datas, *J. Acoust. Soc. Am.*, **103** 2901.
[15] Martinez L., Morvan B., Izbicki J.L., 2003, Phonon localisation methods through time and space: experimental SAW phonon aspects on a cylindrical shell, *J. Acoust. Soc. Am.*, **113** 2294.
[16] Leclaire P., Goossens J., Martinez L., Wilkie-Chancellier N., Serfaty S., Glorieux C., 2006, Study of the bending modes in circular quartz resonators, *IEEE Trans. UFFC*, **53(10)**, 1934-1943.
[17] Lee P.C.Y., Liu N., 2004, Plane harmonic waves in an infinite piezoelectric plate with dissipation, *IEEE Trans. UFFC*, **51 (12),** 1629–1638.
[18] Martinez L., Wilkie-Chancellier N., Glorieux C., 2008, 3D Gabor analysis of transient space-time waves, *J. Acoust. Soc. Am.*, **123 (5)** 3432.